Single-exposure optical sectioning by color structured illumination microscopy

Leo G. Krzewina and Myung K. Kim

Department of Physics, University of South Florida, Tampa, Florida 33620

Received September 9, 2005; revised November 17, 2005; accepted November 19, 2005; posted November 22, 2005 (Doc. ID 64704)

Structured illumination microscopy (SIM) is a wide-field technique that rivals confocal microscopy in optical sectioning ability at a small fraction of the acquisition time. For standard detectors such as a CCD camera, SIM requires a minimum of three sequential frame captures, limiting its usefulness to static objects. By using a color grid and camera, we surpass this limit and achieve optical sectioning with just a single image acquisition. The extended method is now applicable to moving objects and improves the speed of three-dimensional imaging of static objects by at least a factor of three. © 2006 Optical Society of America

OCIS codes: 180.6900, 110.0180, 110.6880.

In many physical and life science applications, the conventional light microscope suffers a loss of clarity when in-focus features are obscured by defocused neighboring regions. In recent years, instruments capable of optical sectioning have been developed to overcome this limitation. The confocal scanning microscope is a well-known example that has proved invaluable, but due to its pointwise light structure it must be scanned both laterally and longitudinally to obtain a complete three-dimensional image. The much faster method of structured illumination microscopy (SIM) proposed by Neil *et al.*[1] introduces a moving sinusoidal linear grating into the illumination path and after straightforward computer processing yields optical sectioning with just three image acquisitions per axial position. The grating motion must be precisely synchronized with the camera to ensure a proper phase difference between frames, implying that the object must remain stationary over a time scale that is typically limited by the camera frame rate. With special hardware,[2] the total acquisition time may be reduced enough to apply SIM to moving objects, but this is relatively expensive. Here, we exploit the red, green, and blue (RGB) channels of the color camera to combine the three separate captures by replacing the moving monochromatic grid with a fixed color grid. With this simple scheme, the three phase offset images are captured in parallel. Because a color grid is used, we refer to this as color SIM (CSIM).

The experimental setup is shown in Fig. 1. Incoherent light from a high-intensity white LED is directed toward the grid in a Kohler illumination arrangement. The structured light passes through a nonpolarizing beam splitter to be focused by an Edmund Optics microscope objective ($10\times/0.25$ NA tube length corrected) onto the object. Light scattered by the object passes back through the microscope objective and beam splitter and is imaged onto the camera, a Sony XCD-X710CR color camera with a Bayer filter, for later processing. The grid and camera are both conjugate to the object, and the magnification β of the system is defined as the magnification from the object to the grid plane. Throughout this Letter, $\beta = 15.5$, and the object field size is $240\ \mu\text{m} \times 180\ \mu\text{m}$ imaged onto an 800×600 CCD array.

As the grid is of prime importance, we will discuss it in some detail. In standard SIM, a sinusoidal grating yields a fringe pattern $S_i(x)$ of the approximate form

$$S_i(x) = 1 + m \cos\left(\frac{2\pi x}{T} + \phi_i\right). \quad (1)$$

Here the spatial period of the grid at the object is given by

$$T = T_0/\beta, \quad (2)$$

where T_0 is the unmagnified grid period and m is the modulation depth. Images having intensity $I_i(x,y)$ are captured for the three phase offsets $\phi_1 = 0$, $\phi_2 = 2\pi/3$, and $\phi_3 = 4\pi/3$. It can be shown[1] that the optically sectioned image of interest may be obtained from

$$I_{\text{sectioned}} = [(I_1 - I_2)^2 + (I_2 - I_3)^2 + (I_1 - I_3)^2]^{1/2}. \quad (3)$$

Apparently the indices $i = \{1,2,3\}$ can be replaced with color channels RGB, provided that the responses of the channels are separable. To simplify the separation procedure and to increase light efficiency, we adopt a rectangular rather than a sinusoidal grid, for which the artifact ramifications have been de-

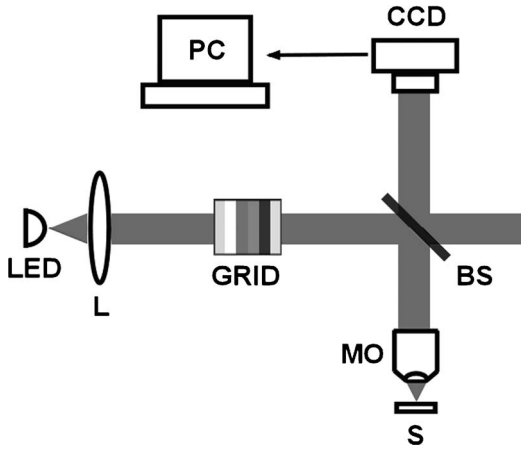

Fig. 1. Experimental setup: L, collimating lens; GRID, slide of the color grid pattern; BS, beam splitter; MO, microscope objective ($10\times/0.25$ NA); S, sample.

0146-9592/06/040477-3/$15.00

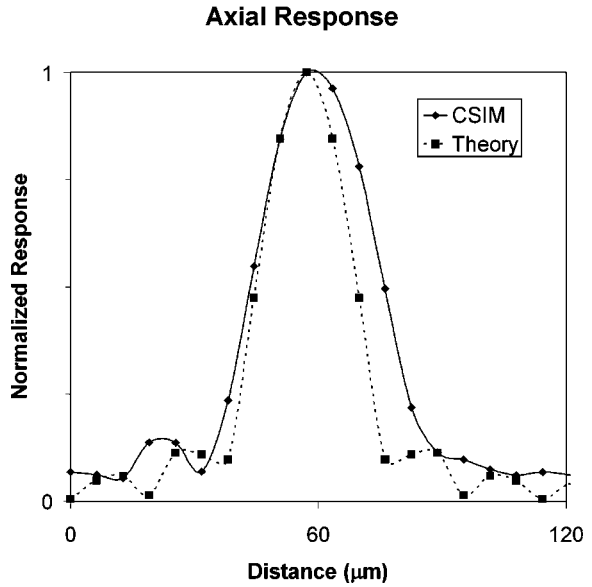

Fig. 2. CSIM normalized axial response with a plane mirror object (solid curve) and the theoretical response calculated from Eq. (10) of Ref. 1 (dashed curve).

scribed previously.[3,4] This implies a grid composed of a repeating pattern of six equally spaced stripes: green, yellow, red, magenta, blue, and cyan.

The color grids were provided by Sprint Multimedia, Inc., of Tampa, Florida, as 35 mm slides. The claimed print resolution of 10.6 μm per line implies a minimum T_0 of 63.6 μm, but we found this grid size to be too noisy. For the data presented here we used $T_0 = 254.4$ μm ($T = 16.4$ μm at the object) and note that by adjusting β a smaller value of T may be obtained, as seen from Eq. (2).

The system is calibrated by finding the color values on the slides that lead to the desired levels at the camera and by measuring constants used in color-decoupling equations. The generic spectral response is obtained by calibrating to a planar mirror object; for other objects, the individual response will be considered during postprocessing. Given raw image color channel intensities I_R^0, I_G^0, and I_B^0, we assume a first-order linear correction (with $\alpha_{xy} \geq 0$):

$$I_R = + \alpha_{RR} I_R^0 - \alpha_{RG} I_G^0 - \alpha_{RB} I_B^0,$$

$$I_G = - \alpha_{GR} I_R^0 + \alpha_{GG} I_G^0 - \alpha_{GB} I_B^0,$$

$$I_B = - \alpha_{BR} I_R^0 - \alpha_{BG} I_G^0 + \alpha_{BB} I_B^0. \quad (4)$$

By adjusting the levels on the 35 mm slides, we were able to use $\alpha_{xx} \equiv 1$. The other calibration constants were found by measuring the response to various levels of $R+G$, $R+B$, and $G+B$. For example, $\partial G / \partial R = \alpha_{GR}$ was found from the change in measured green intensity for two slides having different red levels. The raw camera RGB data are thus roughly corrected for color mixing in the light source, slides, and camera. To compensate for object color, we also balance the channels by scaling I_R, I_G, and I_B to their maximum average value. This is equivalent to the uniform intensity normalization approach used by Cole *et al.*[4] for SIM, a straightforward postprocessing technique that substantially reduces linear artifacts.

For CSIM to be successful, its optical sectioning ability must be comparable with that of standard SIM. The system response to an axially translated planar mirror is shown in Fig. 2, along with the theoretical curve from Eq. (10) of Ref. 1, using $\lambda = 550$ nm in the normalized spatial frequency expression $\tilde{\nu} = \beta \lambda \nu / \mathrm{NA}$, with $\nu = T_0^{-1}$. The FWHM of the responses from theory and our experiment are 24.2 and 32.6 μm, respectively. This apparently low sectioning strength scales as β^{-1} and should also improve with optimized combination of lamp, grid, and camera. Our experimental curve exhibits the same asymmetry and broadening as that of Mitić *et al.*,[2] which was attributed to longitudinal chromatic aberration. Since theory predicts only a 0.6 μm difference between the FWHM calculated at $\lambda = 450$ and at $\lambda = 650$ nm (monochromatic, with other parameters the same), the broadening in our result is likely due to spherical and chromatic aberrations from our microscope objective and collimating lens, which are not planar corrected. Additionally, the 35 mm film has varying surface curvature due to its fabrication method.

The effectiveness of our microscope is demonstrated in Fig. 3, in which a moth abdomen is shown. A total volume of 240 μm $\times$ 180 μm $\times$ 229 μm was scanned in nine axial steps of size $\delta z = 25.4$ μm, so exactly ten images were acquired. The conventional view in Fig. 3(a) shows little of the hair structure in a single frame taken from midway along the scan. The autofocus image in Fig. 3(b) is composed from the brightest pixels from all ten sections. One particular section is shown in Fig. 3(c). A height map may also be constructed from the raw data, as in Fig. 3(d), which has ten gray-scale levels indicating the z position of the various features. For instance, the bright region in the upper right of 3(b) is actually recessed, as seen in Fig. 3(d).

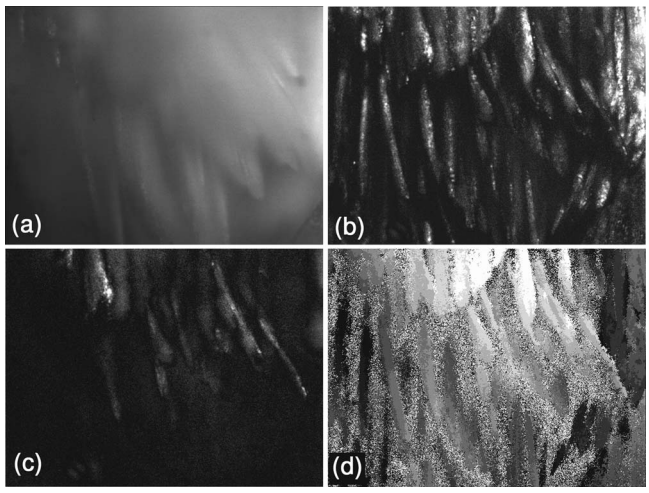

Fig. 3. Moth abdomen. (a) Single conventional image taken midway along z. (b) CSIM autofocus image composed from the brightest pixels in the ten sections. (c) Single CSIM section. (d) Height map in which gray levels correspond to each axial position.

Since application of CSIM to moving objects depends on widely varying camera exposure time and magnification β, the ability to estimate the maximum object velocity given these parameters is desirable. First, consider the transverse motion direction for the worst case of velocity perpendicular to the grid lines. Although it is not difficult to derive an analytical estimation for $v_{\max,\perp}$, we present results from a simulation in which we found an approximately linear response:

$$R = \begin{cases} 1 - \dfrac{\Delta\phi}{2\pi} = 1 - \dfrac{vt}{T}, & vt < T \\ 0, & vt \geqslant T \end{cases}. \tag{5}$$

Here R is the normalized integrated response for a total phase shift $\Delta\phi$ of the grid at the object as a result of either grid or object motion with relative velocity v during exposure time t. For slow enough objects with $\Delta\phi$ that do not exceed one period and if we require a response $R \geqslant 0.5$, Eq. (5) is solved for v to find

$$v_{\max,\perp} = T_0/2\beta t. \tag{6}$$

Equation (6) is physically intuitive and readily employed. For example, for the pollen grain in Ref. 1 with $T_0 = 25$ μm and $\beta = 13.9$, assuming an exposure time of $t = 0.001$ s, the maximum velocity is 900 μm/s. This is a high velocity considering the field size of only 100 μm $\times$ 70 μm.

The maximum observable axial velocity $v_{\max,\parallel}$ remains to be determined. We turn again to Eq. (10) from Ref. 1, which may be solved graphically for $R = 0.5$ (e.g., with Mathematica) to observe the solution behavior in terms of T_0 and β. The key here is to require that the object stays within the FWHM axial range during the exposure time:

$$\Delta z = \mathrm{FWHM} = v_{\max,\parallel} t. \tag{7}$$

While Eqs. (6) and (7) give velocities for which the system can function, other constraints, such as contiguous sectioning, may require slower translation as limited by the camera frame rate.

To conclude, we have summarized the strengths and weaknesses of CSIM. By requiring only a single camera capture to achieve optical sectioning, it is possible to obtain sectioned images of moving objects. For static objects, a complete volume may be constructed with just one image per axial position, and since the translator does not need to stop for each δz, the total acquisition time will be reduced by more than a factor of 3. Since no grid actuator is needed, the microscope setup is simplified, and phase offset artifacts are eliminated. The 35 mm slides are readily available and very inexpensive. As for negative points, it takes some effort to properly calibrate the system to the lamp spectrum and camera spectral response to obtain a custom-made grid. Improved results are to be expected from higher-quality grids, as the 35 mm slides suffer from noise and nonuniformities—one candidate for an upgraded grid is dielectric film.[5] Even after calibration, color inherent to the object may introduce linear artifacts. Postprocessing[3,4] and color filters help minimize this problem. The lamp must be carefully chosen to provide both optimal color channel separation and light intense enough to take advantage of the brief exposure times available in CSIM. Since the light efficiency is reduced through grid filtering by approximately a factor of ten (the lamp-to-stripe bandwidth ratio), the use of a bright lamp or a sensitive camera is needed for applicability of this method.

We thank Sprint Multimedia for providing the color grids, often as quickly as overnight, and Bill Sargent for photography advice. This work is supported in part by a grant from the National Science Foundation.

References

1. M. A. A. Neil, R. Juskaitis, and T. Wilson, Opt. Lett. **22**, 1905 (1997).
2. J. Mitić, T. Anhut, M. Meier, M. Ducros, A. Serov, and T. Lasser, Opt. Lett. **28**, 698 (2003).
3. L. H. Schaefer, D. Schuster, and J. Schaffer, J. Microsc. (Oxford) **216**, 165 (2004).
4. M. J. Cole, J. Siegel, S. E. D. Web, R. Jones, K. Dowling, Mj. J. Dayel, D. Parsons-Karavassilis, P. M. W. French, M. J. Lever, L. O. D. Sucharov, M. A. A. Neil, R. Juskaitis, and T. Wilson, J. Microsc. (Oxford) **203**, 246 (2001).
5. J. Kvavle, C. Bell, J. Henrie, S. Schultz, and A. Hawkins, Opt. Express **12**, 5789 (2004).